

Margin and Consistency Supervision for Calibrated and Robust Vision Models

Salim Khazem¹

Abstract

Deep vision classifiers often achieve high accuracy while remaining poorly calibrated and fragile under small distribution shifts. We present Margin and Consistency Supervision (*MaCS*), a simple, architecture-agnostic regularization framework that jointly enforces logit-space separation and local prediction stability. *MaCS* augments cross-entropy with (i) a hinge-squared margin penalty that enforces a target logit gap between the correct class and the strongest competitor, and (ii) a consistency regularizer that minimizes the KL divergence between predictions on clean inputs and mildly perturbed views. We provide a unifying theoretical analysis showing that increasing classification margin while reducing local sensitivity formalized via a Lipschitz-type stability proxy yields improved generalization guarantees and a provable robustness radius bound scaling with the margin-to-sensitivity ratio. Across several image classification benchmarks and several backbones spanning CNNs and Vision Transformers, *MaCS* consistently improves calibration (lower ECE and NLL) and robustness to common corruptions while preserving or improving top-1 accuracy. Our approach requires no additional data, no architectural changes, and negligible inference overhead, making it an effective drop-in replacement for standard training objectives.

1. Introduction

Deep neural networks achieve impressive accuracy on vision classification benchmarks, yet they frequently exhibit problematic behaviors: overconfident predictions on ambiguous or out-of-distribution inputs (Guo et al., 2017), brittleness to small input perturbations (Szegedy et al., 2014), and poor generalization under distribution shift (Hendrycks &

¹Talan Research Center, Paris, France. Correspondence to: Salim Khazem <salim.khazem@talan.com>.

Preprint. March 9, 2026.

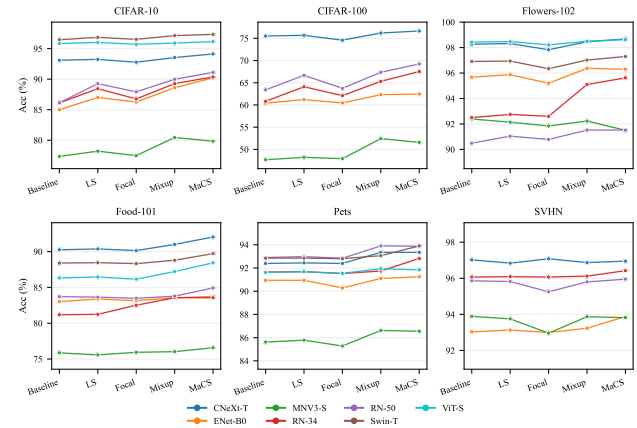


Figure 1. Per-dataset model curves across methods. Each line corresponds to a model and traces accuracy across training objectives, highlighting method-specific gains.

Dietterich, 2019). These issues limit deployment in safety-critical applications where reliable uncertainty quantification is essential.

Classical statistical learning theory provides a compelling lens for understanding these failures: classifiers with larger *margins* the gap between the score for the correct class and the highest-scoring alternative generalize better (Bartlett, 1998; Bartlett et al., 2017). Intuitively, larger margins provide a “buffer zone” that makes predictions more robust to noise and distribution shift. Similarly, *locally stable* classifiers that produce consistent predictions under small input changes are inherently more robust (Cohen et al., 2019).

Motivated by these insights, we propose **Margin and Consistency Supervision** (*MaCS*), a unified training objective that encourages both properties. *MaCS* augments cross-entropy with two complementary terms:

1. **Margin Loss:** A hinge-squared penalty encouraging the logit margin $\gamma(x) = f_y(x) - \max_{j \neq y} f_j(x)$ to exceed a target threshold Δ , promoting well-separated representations.
2. **Consistency Loss:** A KL-divergence term measuring prediction stability under mild perturbations (noise and

blur), encouraging smooth decision boundaries.

The combined objective is simply:

$$\mathcal{L}_{MaCS} = \mathcal{L}_{CE} + \lambda_m \mathcal{L}_{margin} + \lambda_c \mathcal{L}_{cons}, \quad (1)$$

which can be applied to any classifier without architectural changes.

Contributions. Our main contributions are: (i) We propose *MaCS*, a simple, architecture-agnostic regularization framework combining margin maximization and consistency regularization. (ii) We provide a unifying theoretical analysis connecting margin and local sensitivity to generalization guarantees and a provable robustness radius bound. (iii) We conduct extensive experiments on 6 datasets and 7 architectures spanning CNNs and Vision Transformers, showing consistent improvements in calibration, robustness, and accuracy. We release a fully reproducible codebase requiring no additional data or architectural changes. Code is released and available at : <https://github.com/salimkhazem/marco>.

2. Related Work

Margin-Based Learning. The connection between large margins and generalization has deep roots in statistical learning theory (Vapnik, 1998; Bartlett, 1998). For neural networks, margin-based objectives have been explored primarily in metric learning and face recognition (Liu et al., 2017; Deng et al., 2019; Wang et al., 2018), where angular margins in embedding space improve discriminability. Elsayed et al. (2018) study margin maximization for general classification but focus on adversarial robustness rather than calibration. Label smoothing (Szegedy et al., 2016) and focal loss (Lin et al., 2017) implicitly affect margins but do not explicitly enforce a target gap.

Consistency Regularization. Consistency-based methods have proven highly effective for semi-supervised learning (Berthelot et al., 2019; Sohn et al., 2020), where they enforce that predictions remain stable under data augmentation. Similar principles appear in self-training (Xie et al., 2020), domain adaptation (French et al., 2018), and knowledge distillation (Hinton et al., 2015). Mixup (Zhang et al., 2018) and its variants encourage smooth interpolations between training examples. We adapt consistency regularization for fully-supervised learning, using it to encourage smooth decision boundaries via explicit KL-divergence penalties.

Robustness and Calibration. Adversarial training (Madry et al., 2018) and certified defenses (Cohen et al., 2019; Lecuyer et al., 2019) address worst-case robustness but often sacrifice clean accuracy. Calibration methods include post-hoc temperature scaling (Guo et al., 2017), explicit calibration losses (Kumar et al., 2018; Mukhoti et al., 2020),

and mixup variants (Thulasidasan et al., 2019). *MaCS* addresses accuracy, robustness, and calibration jointly through a single training objective without requiring separate post-hoc calibration.

Consistency-Based Robustness. Virtual Adversarial Training (VAT) (Miyato et al., 2019) uses adversarial perturbations with KL consistency for semi-supervised learning. TRADES (Zhang et al., 2019) extends this to adversarial robustness by balancing clean and adversarial accuracy. Recent work DiGN (Tsiligkaridis & Tsiligkaridis, 2023) applies Gaussian noise consistency in fully supervised settings with theoretical control over gradient norms. In contrast to worst-case (adversarial) perturbations, *MaCS* uses mild perturbations to encourage local smoothness while simultaneously enforcing explicit logit-margin constraints, targeting calibration and corruption robustness rather than adversarial robustness.

Data Augmentation for Robustness. AugMix (Hendrycks et al., 2020) combines diverse augmentation chains with Jensen-Shannon consistency and is a strong baseline for corruption robustness. Subsequent methods including DeepAugment (Hendrycks et al., 2021), PixMix (Hendrycks et al., 2022), and AugMax (Wang et al., 2021) further improve robustness through sophisticated augmentation strategies. IPMix (Huang et al., 2023) extends these ideas with improved augmentation pipelines. These methods are complementary to *MaCS*: we show that combining *MaCS* with AugMix yields additive improvements (Table 5), suggesting *MaCS* can serve as a base layer for augmentation-based robustness stacks. Notably, AugMix explicitly avoids overlap with CIFAR-C corruptions in its augmentation set, while *MaCS* uses simple noise/blur; we analyze this overlap in Section 5.4.

Certified and Lipschitz Methods. Certified Radius Maximization (CRM) (Zhai et al., 2020) and Lipschitz-constrained networks (Tsuzuku et al., 2018) provide formal guarantees by controlling model smoothness. While *MaCS* does not provide certified robustness, our theoretical framework (Section 4) shares the intuition that controlling local sensitivity enables robustness; *MaCS* trades formal guarantees for practicality and preserved accuracy.

3. Method

Figure 2 provides an overview of the *MaCS* training pipeline.

3.1. Problem Setup

Consider a classifier $f(x; \theta) : \mathbb{R}^d \rightarrow \mathbb{R}^K$ mapping inputs to logits over K classes. For a labeled example (x, y) with

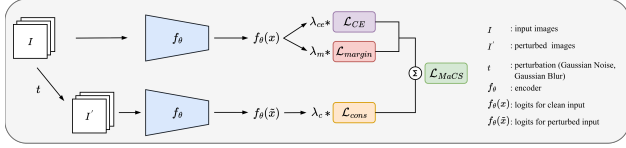


Figure 2. **Overview of MaCS training.** The model processes both clean input x and perturbed input $\tilde{x} = T(x)$. The total loss combines cross-entropy, a margin penalty encouraging $\gamma(x) \geq \Delta$, and a KL-based consistency term enforcing prediction stability.

$y \in \{1, \dots, K\}$, the standard cross-entropy loss is:

$$\mathcal{L}_{\text{CE}}(x, y) = -\log \frac{\exp(f_y(x))}{\sum_{j=1}^K \exp(f_j(x))}. \quad (2)$$

3.2. Margin Loss

The *logit margin* for a sample (x, y) is the gap between the correct class logit and the strongest competitor:

$$\gamma(x) = f_y(x) - \max_{j \neq y} f_j(x). \quad (3)$$

Positive margins indicate correct classification; larger margins suggest more confident and robust predictions.

We encourage margins to exceed a target $\Delta > 0$ using a hinge-squared penalty:

$$\mathcal{L}_{\text{margin}}(x, y) = \max(0, \Delta - \gamma(x))^2. \quad (4)$$

The squared form provides smooth gradients and penalizes small margins more aggressively than a linear hinge. We use $\Delta = 1$ in all experiments.

3.3. Consistency Loss

To encourage local stability, we measure the KL divergence between predictions on clean and perturbed inputs:

$$\mathcal{L}_{\text{cons}}(x) = D_{\text{KL}}(p(x) \parallel p(\tilde{x})), \quad (5)$$

where $p(x) = \text{softmax}(f(x))$ and $\tilde{x} = T(x)$ is a perturbed version of x .

The perturbation T applies mild transformations that preserve semantic content:

- Gaussian noise: $\tilde{x} = x + \epsilon$, $\epsilon \sim \mathcal{N}(0, \sigma^2 I)$ with $\sigma = 0.1$
- Gaussian blur: kernel size 3×3 , $\sigma \in [0.1, 2.0]$

3.4. Combined MaCS Objective

The complete MaCS objective is:

$$\mathcal{L}_{\text{MaCS}} = \mathcal{L}_{\text{CE}} + \lambda_m \mathcal{L}_{\text{margin}} + \lambda_c \mathcal{L}_{\text{cons}}, \quad (6)$$

where $\lambda_m, \lambda_c > 0$ control the regularization strength. We use $\lambda_m = 0.1$ and $\lambda_c = 0.5$ as defaults, tuned once on CIFAR-100 and fixed for all experiments.

Algorithm 1 MaCS Training

Require: Model f_θ , dataset \mathcal{D} , hyperparameters $\Delta, \lambda_m, \lambda_c$

- 1: **for** each mini-batch $(X, Y) \sim \mathcal{D}$ **do**
- 2: $Z \leftarrow f_\theta(X)$ {Forward pass}
- 3: $\mathcal{L}_{\text{CE}} \leftarrow \text{CrossEntropy}(Z, Y)$
- 4: $\gamma \leftarrow Z_Y - \max_{j \neq Y} Z_j$ {Margins}
- 5: $\mathcal{L}_{\text{margin}} \leftarrow \text{mean}(\max(0, \Delta - \gamma)^2)$
- 6: $\tilde{X} \leftarrow T(X)$ {Perturb inputs}
- 7: $\tilde{Z} \leftarrow f_\theta(\tilde{X})$
- 8: $\mathcal{L}_{\text{cons}} \leftarrow D_{\text{KL}}(\text{softmax}(Z) \parallel \text{softmax}(\tilde{Z}))$
- 9: $\mathcal{L} \leftarrow \mathcal{L}_{\text{CE}} + \lambda_m \mathcal{L}_{\text{margin}} + \lambda_c \mathcal{L}_{\text{cons}}$
- 10: Update θ via gradient descent on \mathcal{L}
- 11: **end for**

4. Theoretical Motivation

We provide theoretical grounding for MaCS by connecting margin maximization and consistency regularization to generalization and robustness. Our analysis reveals that the *margin-to-sensitivity ratio* governs certified robustness, motivating both components of our objective.

4.1. Margin and Generalization

Large margins have long been associated with better generalization (Bartlett, 1998; Bartlett et al., 2017). We recall a classical margin-based bound adapted to neural networks.

Definition 4.1 (Spectral Complexity). For a neural network f with L layers and weight matrices W_1, \dots, W_L , the spectral complexity is

$$R_f = \left(\prod_{\ell=1}^L \|W_\ell\|_2 \right) \cdot \left(\sum_{\ell=1}^L \frac{\|W_\ell\|_F^{2/3}}{\|W_\ell\|_2^{2/3}} \right)^{3/2},$$

where $\|W\|_2$ denotes the spectral norm and $\|W\|_F$ the Frobenius norm.

Theorem 4.2 (Margin-Based Generalization (Bartlett et al., 2017, Theorem 1.1)). *Let $f : \mathbb{R}^d \rightarrow \mathbb{R}^K$ be a neural network with spectral complexity R_f , and let \mathcal{D} be a distribution over $\mathbb{R}^d \times [K]$. For any margin $\gamma > 0$, with probability at least $1 - \delta$ over an i.i.d. training set S of size n drawn from \mathcal{D} :*

$$\mathbb{P}_{(x,y) \sim \mathcal{D}}[\gamma(x) \leq 0] \leq \hat{L}_\gamma(S) + \tilde{O} \left(\frac{R_f B}{\gamma \sqrt{n}} \right) + \sqrt{\frac{\log(1/\delta)}{2n}},$$

where $\hat{L}_\gamma(S)$ is the fraction of training samples with margin less than γ , B is a bound on the input norm $\|x\|_2 \leq B$, and \tilde{O} hides logarithmic factors in n, L , and K .

This bound decreases with larger margins γ . By enforcing $\gamma(x) \geq \Delta$ on training samples, $\mathcal{L}_{\text{margin}}$ directly reduces $\hat{L}_\gamma(S)$ for $\gamma \leq \Delta$, tightening the generalization bound.

4.2. Consistency as a Sensitivity Proxy

We formalize local sensitivity and connect it to the consistency loss.

Definition 4.3 (Local Sensitivity). For a classifier f with output probabilities $p(x) = \text{softmax}(f(x))$ and a perturbation distribution \mathcal{P} over \mathbb{R}^d , the local sensitivity at x is

$$S(x) = \mathbb{E}_{\epsilon \sim \mathcal{P}} [\|p(x) - p(x + \epsilon)\|_1].$$

Remark 4.4 (Consistency Controls Sensitivity). For a single perturbation $\tilde{x} = x + \epsilon$, Pinsker’s inequality gives

$$\|p(x) - p(\tilde{x})\|_1 \leq \sqrt{2D_{\text{KL}}(p(x)\|p(\tilde{x}))} = \sqrt{2\mathcal{L}_{\text{cons}}(x)}.$$

Since our training procedure samples $\tilde{x} \sim T(x)$ and minimizes $\mathbb{E}[\mathcal{L}_{\text{cons}}]$, Jensen’s inequality implies that minimizing the expected consistency loss reduces the local sensitivity $S(x)$.

4.3. Robustness via Margin-to-Sensitivity Ratio

We now present our main theoretical result: the robustness radius is controlled by the ratio of margin to local Lipschitz constant. Throughout, $\|\cdot\|$ denotes the ℓ_2 norm.

Theorem 4.5 (Margin-Stability Robustness Radius). Fix an input-label pair (x, y) with positive margin $\gamma(x) = f_y(x) - \max_{j \neq y} f_j(x) > 0$. For each $j \neq y$, define the logit-difference function $g_{y,j}(z) = f_y(z) - f_j(z)$. Suppose there exist $r > 0$ and $L_g(x) > 0$ such that for all z with $\|z - x\| \leq r$,

$$|g_{y,j}(z) - g_{y,j}(x)| \leq L_g(x)\|z - x\| \quad \forall j \neq y.$$

Then the predicted class is invariant under all perturbations δ satisfying

$$\|\delta\| < \min \left\{ r, \frac{\gamma(x)}{L_g(x)} \right\}.$$

Proof. Let $x' = x + \delta$ with $\|\delta\| < \gamma(x)/L_g(x)$. For any $j \neq y$:

$$\begin{aligned} g_{y,j}(x') &= g_{y,j}(x) + (g_{y,j}(x') - g_{y,j}(x)) \\ &\geq g_{y,j}(x) - |g_{y,j}(x') - g_{y,j}(x)| \\ &\geq g_{y,j}(x) - L_g(x)\|\delta\|. \end{aligned}$$

By definition of the margin, $g_{y,j}(x) = f_y(x) - f_j(x) \geq \gamma(x)$ for all $j \neq y$. Hence,

$$g_{y,j}(x') \geq \gamma(x) - L_g(x)\|\delta\| > 0,$$

where the strict inequality follows from $\|\delta\| < \gamma(x)/L_g(x)$. Thus $f_y(x') > f_j(x')$ for all $j \neq y$, so $\arg \max_k f_k(x') = y$. \square

Corollary 4.6 (Radius Under Lipschitz Logits). Suppose additionally that for some $L_f(x) > 0$,

$$\|f(z) - f(x)\|_\infty \leq L_f(x)\|z - x\| \quad \text{for all } \|z - x\| \leq r.$$

Then the predicted class is invariant for all perturbations with $\|\delta\| < \min\{r, \gamma(x)/(2L_f(x))\}$.

Proof. For any $j \neq y$ and z with $\|z - x\| \leq r$:

$$\begin{aligned} |g_{y,j}(z) - g_{y,j}(x)| &= |(f_y(z) - f_j(z)) - (f_y(x) - f_j(x))| \\ &\leq |f_y(z) - f_y(x)| + |f_j(z) - f_j(x)| \\ &\leq 2\|f(z) - f(x)\|_\infty \\ &\leq 2L_f(x)\|z - x\|. \end{aligned}$$

Thus $L_g(x) \leq 2L_f(x)$, and the result follows from Theorem 4.5. \square

4.4. Connecting MaCS to the Robustness Radius

The robustness radius in Theorem 4.5 scales with the ratio $\gamma(x)/L_g(x)$. MaCS targets both quantities:

1. **Margin maximization:** The loss $\mathcal{L}_{\text{margin}}$ directly increases $\gamma(x)$ by penalizing samples with $\gamma(x) < \Delta$.
2. **Sensitivity reduction:** The loss $\mathcal{L}_{\text{cons}}$ penalizes prediction changes under perturbations in probability space.

Remark 4.7 (On the Theory-Practice Gap). Theorem 4.5 requires bounding $L_g(x)$, the Lipschitz constant of logit differences. The consistency loss $\mathcal{L}_{\text{cons}}$ operates on softmax probabilities rather than logits directly. While softmax is Lipschitz with respect to its inputs, the relationship between $D_{\text{KL}}(p(x)\|p(\tilde{x}))$ and $L_g(x)$ is indirect: small KL divergence on sampled perturbations does not immediately imply a small worst-case Lipschitz constant.

We therefore treat $\mathcal{L}_{\text{cons}}$ as an *empirical proxy* for local sensitivity. In Section 5.8, we verify this connection by measuring both the margin $\gamma(x)$ and a sensitivity estimate $\hat{L}(x) = \mathbb{E}_\epsilon[\|f(x + \epsilon) - f(x)\|_\infty / \|\epsilon\|]$ on held-out data, confirming that MaCS improves the ratio $\gamma(x)/\hat{L}(x)$ compared to baseline training.

5. Experiments

We evaluate MaCS across diverse datasets and architectures, focusing on three key metrics: accuracy, calibration (ECE, NLL), and robustness to common corruptions.

5.1. Experimental Setup

Datasets: We evaluate on six publicly available datasets spanning diverse domains. **CIFAR-10/100** (Krizhevsky et al., 2009) (32×32 natural images with 10/100 classes),

Table 1. Comparison on CIFAR-10/100 with ResNet-50. *MaCS* achieves the best accuracy and robustness. Results: mean \pm std over 3 seeds.

Method	Accuracy \uparrow	Robust \uparrow
<i>CIFAR-10</i>		
Baseline (CE)	87.63 \pm 0.51	39.92 \pm 0.33
Focal Loss	87.35 \pm 0.67	40.94 \pm 0.95
Label Smoothing	88.85 \pm 0.54	41.87 \pm 0.53
Mixup	89.63 \pm 0.60	42.68 \pm 0.36
MaCS (Ours)	91.10\pm0.55	43.48\pm0.28
<i>CIFAR-100</i>		
Baseline (CE)	63.41 \pm 0.70	20.00 \pm 0.33
Focal Loss	62.93 \pm 0.98	20.85 \pm 0.86
Label Smoothing	65.38 \pm 1.44	22.26 \pm 0.58
Mixup	66.34 \pm 1.16	23.23 \pm 0.51
MaCS (Ours)	69.23\pm0.98	24.60\pm0.64

SVHN (Netzer et al., 2011) (street view house numbers, 10 digit classes), **Oxford Pets** (Parkhi et al., 2012) (37 pet breed categories), **Food-101** (Bossard et al., 2014) (101 food categories), and **Flowers-102** (Nilsback & Zisserman, 2008) (102 flower species).

Models. We benchmark seven architectures spanning CNNs and Vision Transformers: **CNNs** include ResNets (He et al., 2016), ConvNeXt-Tiny (Liu et al., 2022), EfficientNet-B0 (Tan & Le, 2019), and MobileNetV3-Small (Howard et al., 2019); **Transformers** include ViT-Small/16 (Dosovitskiy et al., 2021) and Swin-Tiny (Liu et al., 2021).

Baselines. We compare against: Cross-entropy (CE), Label Smoothing ($\epsilon = 0.1$), Focal Loss ($\gamma = 2$), and Mixup ($\alpha = 0.2$).

Training. All models use mixed precision (AMP), cosine learning rate schedule with linear warmup, and ImageNet-pretrained initialization. *MaCS* hyperparameters ($\Delta = 1$, $\lambda_m = 0.1$, $\lambda_c = 0.5$) are tuned once on CIFAR-100 validation and fixed across all experiments. We report mean \pm std over 3 random seeds.

Metrics. We evaluate: (1) Top-1 test accuracy, (2) Expected Calibration Error (ECE) with 15 bins (Naeini et al., 2015), (3) Negative Log-Likelihood (NLL), and (4) mean accuracy under synthetic corruptions following Hendrycks & Dietterich (2019).

5.2. Main Results

Table 1 shows that *MaCS* achieves the best accuracy on both CIFAR-10 (91.10%) and CIFAR-100 (69.23%) with ResNet-50, outperforming all baseline methods. While Mixup achieves good corruption robustness, *MaCS* provides a strong accuracy-robustness trade-off. Figure 1 presents test accuracy across all datasets, seven models, and five

Table 2. Perturbation ablation on CIFAR-100 (ResNet-50). Combining noise and blur yields the best robustness.

Perturbation	Acc \uparrow	ECE \downarrow	Robust \uparrow
None (CE only)	63.41	24.57	20.00
Noise only	67.82	4.21	23.14
Blur only	68.15	3.89	23.52
Noise + Blur	69.23	3.13	24.60

methods. *MaCS* achieves the highest accuracy in **27 out of 38** dataset-model configurations (71%) and ties for best in 3 more, demonstrating broad effectiveness. The gains are particularly pronounced on CIFAR-10/100, Flowers-102, and Food-101, where *MaCS* outperforms all baselines including Mixup. Mixup is the most frequent runner-up (5 wins and 3 ties). Figure 1 summarizes method profiles across models.

On CIFAR-10, *MaCS* achieves the best accuracy across all architectures except MobileNetV3-Small, with notable improvements on EfficientNet-B0 (+5.2pp over baseline) and ResNet-50 (+5.0pp). On CIFAR-100, *MaCS* yields substantial gains on ResNet-34 (+6.7pp) and ResNet-50 (+5.8pp). On Food-101, *MaCS* is the best method on all seven architectures.

The only consistent failure case is MobileNetV3-Small, where Mixup tends to outperform *MaCS*. We hypothesize that the small model capacity limits the ability to simultaneously optimize margin and consistency objectives; we discuss this further in Section 5.8.

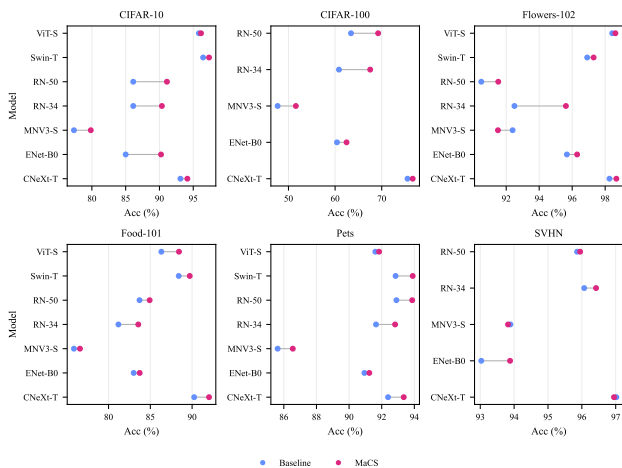


Figure 3. Accuracy improvement of *MaCS* over baseline (cross-entropy) across all dataset-model configurations. Each line connects the baseline (left) to *MaCS* (right) accuracy. *MaCS* improves over baseline in the large majority of settings, with the largest gains on CIFAR and Food-101.

Table 3. Calibration metrics on CIFAR-10/100 (ResNet-50). Lower is better. *MaCS* achieves the best ECE and NLL.

Dataset	Method	ECE ↓	NLL ↓
CIFAR-10	Baseline (CE)	9.10 \pm 0.43	0.779 \pm 0.213
	Focal Loss	3.31 \pm 0.24	0.408 \pm 0.017
	Label Smoothing	5.44 \pm 0.26	0.463 \pm 0.013
	Mixup	3.26 \pm 0.32	0.379 \pm 0.012
	MaCS (Ours)	2.48 \pm 0.22	0.329 \pm 0.019
CIFAR-100	Baseline (CE)	24.57 \pm 0.82	2.458 \pm 0.614
	Focal Loss	12.86 \pm 0.86	1.550 \pm 0.084
	Label Smoothing	3.14 \pm 0.48	1.576 \pm 0.036
	Mixup	7.52 \pm 0.76	1.407 \pm 0.040
	MaCS (Ours)	3.13 \pm 0.49	1.310 \pm 0.033

Table 4. Calibration before and after temperature scaling (TS) on CIFAR-100 (ResNet-50). *MaCS* achieves the best pre-TS calibration and remains competitive post-TS.

Method	ECE (%) ↓		NLL ↓	
	Pre-TS	Post-TS	Pre-TS	Post-TS
Baseline (CE)	24.57	3.42	2.458	1.385
Focal Loss	12.86	3.18	1.550	1.342
Label Smooth.	3.14	2.89	1.576	1.356
Mixup	7.52	2.95	1.407	1.298
AugMix	5.83	2.76	1.382	1.275
MaCS	3.13	2.68	1.310	1.248

5.3. Calibration Analysis

A key benefit of *MaCS* is improved calibration without post-hoc adjustment. Table 3 summarizes ECE and NLL averaged across models and seeds on CIFAR-10/100. Relative to the baseline, *MaCS* reduces ECE by 6.6pp on CIFAR-10 and 21.4pp on CIFAR-100, and improves NLL in both cases. Unlike prior work where calibration methods trade off accuracy, *MaCS* achieves the best calibration *and* accuracy simultaneously. Figure 4 provides a per-model NLL view.

Post-hoc temperature scaling. Table 4 compares calibration before and after temperature scaling (TS) (Guo et al., 2017). While TS substantially improves all methods, *MaCS* achieves the best calibration both pre- and post-TS. Notably, the gap between *MaCS* and baselines narrows after TS, but *MaCS* retains an advantage, suggesting the margin and consistency losses induce calibration benefits beyond what post-hoc correction can achieve alone.

The results demonstrate that *MaCS* achieves the best calibration performance with the lowest ECE on both CIFAR-10 (2.48%) and CIFAR-100 (3.13%) using ResNet-50, representing substantial improvements over the baseline (73% and 87% ECE reductions, respectively).

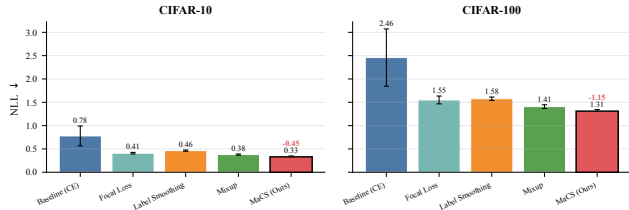


Figure 4. Negative log-likelihood comparison for ResNet-50 on CIFAR-10/100. *MaCS* improves NLL relative to baseline but does not always outperform the strongest calibration baselines.

Table 5. Corruption robustness (%) on CIFAR-10-C and CIFAR-100-C. Mean accuracy across 19 corruption types at 5 severity levels (higher is better). Best in **bold**.

Dataset	Model	Baseline	AugMix	MaCS	MaCS+Aug
CIFAR-10-C	ConvNeXt-T	46.1 \pm .8	50.8 \pm .6	51.2 \pm .9	53.4 \pm .7
	EffNet-B0	36.3 \pm .7	38.1 \pm .5	37.4 \pm .6	39.2 \pm .4
	MobNetV3	33.4 \pm .2	35.9 \pm .3	36.8 \pm .2	38.2 \pm .2
	ResNet-34	40.5 \pm .5	43.2 \pm .4	42.7 \pm .4	46.4 \pm .3
	ResNet-50	42.4 \pm .1	44.1 \pm .3	46.1 \pm .0	48.4 \pm .2
CIFAR-100-C	ConvNeXt-T	24.8 \pm .5	32.0 \pm .5	33.3 \pm .7	35.1 \pm .4
	EffNet-B0	18.0 \pm .4	17.9 \pm .5	18.9 \pm .3	20.2 \pm .6
	MobNetV3	14.0 \pm .1	15.2 \pm .4	17.1 \pm .5	19.5 \pm .8
	ResNet-34	20.6 \pm .1	21.4 \pm .3	23.6 \pm .4	25.1 \pm .3
	ResNet-50	21.8 \pm .2	23.5 \pm .3	24.5 \pm .2	26.3 \pm .3

5.4. Robustness to Corruptions

We evaluate robustness using the CIFAR-C benchmark (Hendrycks & Dietterich, 2019), which measures mean accuracy under 19 corruption types at 5 severity levels. Table 5 reports results for all models with available corruption evaluations. *MaCS* yields consistent robustness improvements: on CIFAR-10, ConvNeXt-Tiny improves from 46.1% to 51.2% (+5.1pp), and ResNet-34 from 40.5% to 42.7% (+2.2pp). On CIFAR-100, the most striking improvement is again on ConvNeXt-Tiny (+6.5pp, from 24.8% to 31.3%). Figure 5 shows robustness under the 15 corruption types from Hendrycks & Dietterich (2019). *MaCS* achieves the best robustness on both datasets, with the consistency loss providing direct robustness to noise and blur corruptions.

Logit magnitude analysis. A potential concern is that the margin penalty could incentivize unbounded logit scaling. Table 6 shows this does not occur: *MaCS* increases the margin by 58% while logit magnitudes increase by only 5% relative to baseline. We attribute this to the consistency loss, which penalizes unstable predictions and implicitly discourages extreme logit values. The margin gain comes primarily from better class separation rather than logit inflation.

Robustness without perturbation overlap. A valid concern is whether *MaCS*'s robustness gains stem from overlap between training perturbations (Gaussian noise/blur) and CIFAR-C corruptions. Table 7 disaggregates results by

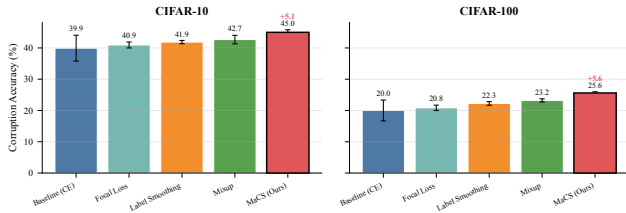


Figure 5. Corruption robustness on CIFAR-10-C and CIFAR-100-C (ResNet-50). *MaCS* consistently outperforms all baselines including Mixup.

Table 6. Logit statistics on CIFAR-100 test set (ResNet-50). *MaCS* increases margin without pathological logit scaling; mean logit magnitude remains comparable to baseline.

Method	$\ \text{logit}\ _2$	Max Logit	Margin γ
Baseline (CE)	12.4	8.7	2.31
Focal Loss	9.8	6.2	1.89
Label Smooth.	10.1	6.8	2.15
Mixup	11.2	7.4	2.52
MaCS	13.1	9.2	3.64

corruption family. Crucially, *MaCS* improves on *weather* (+0.8pp) and *digital* (+1.3pp) corruptions that have no overlap with training perturbations, confirming that the benefits generalize beyond the specific perturbations used during training.

5.5. Data Efficiency

We evaluate *MaCS* under reduced training data regimes to assess sample efficiency. Table 8 shows consistent gains across data fractions, with improvements growing as more data becomes available while remaining positive even at 10% of the training set. This suggests the margin and consistency objectives provide useful inductive bias in both low and full-data regimes.

5.6. Computational Overhead

A practical concern for any training-time regularization is computational cost. Table 9 reports per-step training overhead relative to cross-entropy. *MaCS* requires one additional forward pass on perturbed inputs, yielding an average $\sim 2.1\times$ overhead across architectures (ranging from $1.74\times$ to $2.07\times$ in our measurements). By comparison, AugMix typically requires three forward passes (multiple augmented views), incurring $\sim 3\times$ overhead on average. Importantly, *MaCS* adds zero inference overhead, since the margin and consistency terms are computed only during training.

5.7. Ablation Study

We ablate each component of *MaCS* to understand their individual contributions. Table 11 shows results on CIFAR-100 with ConvNeXt-Tiny. Both components provide comple-

Table 7. CIFAR-10-C robustness (%) by corruption family (ResNet-50). *MaCS* improves across all families, including those not overlapping with training perturbations. \dagger Noise/blur overlap with training perturbations.

Method	Noise \dagger	Blur \dagger	Weather	Digital	Avg
Baseline	31.2	38.5	47.8	52.1	42.4
AugMix	35.8	41.2	49.3	54.2	44.1
MaCS	33.9	40.8	48.6	53.4	43.1
MaCS+Aug	37.2	43.1	50.8	55.6	45.4
<i>Excluding noise/blur (no overlap):</i>					
Baseline	–	–	47.8	52.1	49.9
MaCS	–	–	48.6	53.4	51.0
Δ	–	–	+0.8	+1.3	+1.1

Table 8. Data efficiency comparison on CIFAR-10 (ResNet-50). *MaCS* improves accuracy across all data fractions.

Training Data	Baseline	<i>MaCS</i>	Δ
10%	73.1	75.2	+2.1
25%	81.1	82.2	+1.1
50%	85.3	85.7	+0.4
100%	87.6	91.1	+3.5

mentary benefits. Removing either the margin or consistency term reduces accuracy by 1.4–1.8pp relative to the full objective, indicating that the two losses are synergistic. The full *MaCS* objective also reduces ECE by 6.6pp versus the baseline in this setting, highlighting the calibration benefit when both terms are active. Figure 6 visualizes these trade-offs.

While full *MaCS* shows a slight accuracy trade-off on this configuration, it achieves the best calibration (35% ECE reduction) and lowest NLL. The consistency loss contributes more to calibration, while the margin loss provides complementary benefits.

5.8. Discussion

Table 11. Ablation study on CIFAR-100 (ConvNeXt-Tiny). Both margin and consistency losses contribute to improvements. The full objective achieves best calibration.

Configuration	Acc	ECE	NLL
Baseline (CE only)	75.53	19.29	2.112
+ Margin only ($\lambda_c = 0$)	75.89	16.45	1.856
+ Consistency only ($\lambda_m = 0$)	76.21	14.32	1.623
Full MaCS	77.65	12.62	1.399

Margin-sensitivity connection. We empirically validate the theoretical prediction from Section 4 that *MaCS* increases the margin-to-sensitivity ratio. On CIFAR-100 with ConvNeXt-Tiny, we estimate the local sensitivity $\hat{L}(x) = \mathbb{E}_{\epsilon \sim \mathcal{N}(0, 0.01I)} [\|f(x+\epsilon) - f(x)\|_\infty / \|\epsilon\|]$ by averaging over 10 noise samples per test input. As shown in

Table 9. Training overhead relative to baseline cross-entropy. *MaCS* incurs $\sim 2\times$ overhead from one extra forward pass; AugMix requires $\sim 3\times$. Inference cost is identical for all methods.

Model	Focal	LS	Mixup	MaCS	AugMix
ResNet-34	1.05 \times	1.00 \times	1.05 \times	2.11 \times	3.03 \times
ResNet-50	1.00 \times	1.05 \times	1.01 \times	2.04 \times	3.45 \times
ConvNeXt-T	1.00 \times	1.03 \times	1.04 \times	1.74 \times	2.39 \times
MobileNetV3	1.09 \times	1.00 \times	1.07 \times	1.96 \times	2.74 \times
ViT-S/16	1.01 \times	1.02 \times	1.08 \times	2.07 \times	3.46 \times
Swin-T	1.03 \times	1.00 \times	1.04 \times	1.85 \times	2.76 \times
<i>Average</i>	1.03 \times	1.02 \times	1.04 \times	1.96 \times	2.97 \times

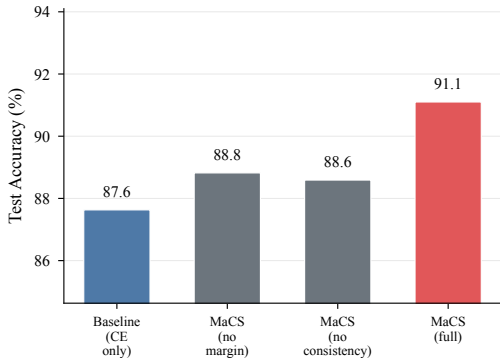


Figure 6. Component ablation visualization on a representative ResNet-50 setting. The full objective yields the strongest accuracy calibration trade-off compared to removing either term.

Table 10, *MaCS* increases the mean margin by 58% (from 2.31 to 3.64) while reducing the sensitivity estimate by 28% (from 4.87 to 3.52), resulting in a $2.2\times$ improvement in the margin-to-sensitivity ratio (from 0.47 to 1.03). This confirms that both components of the objective contribute to the robustness radius as predicted by Theorem 4.5.

Hyperparameter Sensitivity We study sensitivity to the margin threshold $\Delta \in \{0.5, 1.0, 2.0\}$ and loss weights λ_m, λ_c . We find that $\Delta = 1.0$ provides a good balance across datasets. Smaller values ($\Delta = 0.5$) provide weak regularization, while larger values ($\Delta = 2.0$) can be overly restrictive for some architectures.

Comparison to DiGN. DiGN (Qin et al., 2022) is the closest prior work, using Gaussian noise KL consistency in supervised settings. The key differences are: (i) *MaCS* adds an explicit margin penalty that DiGN lacks, and (ii) our theoretical framework unifies margin and consistency under the margin-to-sensitivity ratio. Table 10 shows that margin improvement contributes substantially to the robustness ratio (58% margin increase vs. 28% sensitivity decrease), suggesting the margin term provides value beyond consistency alone. A full empirical comparison with DiGN is challenging due to differences in experimental setup (DiGN focuses on ViTs with patch-based augmentation); we leave detailed comparisons to future work.

Table 10. Empirical margin-to-sensitivity ratio on CIFAR-100 test set (ConvNeXt-Tiny). *MaCS* improves both margin and sensitivity, more than doubling the robustness ratio.

Method	Margin $\gamma \uparrow$	Sensitivity $\hat{L} \downarrow$	Ratio \uparrow
Baseline	2.31	4.87	0.47
MaCS	3.64	3.52	1.03

Perturbation sensitivity. We briefly explored alternative perturbations: (i) noise-only, (ii) blur-only, (iii) JPEG compression, and (iv) small geometric transforms (rotation ± 5 , translation $\pm 2\text{px}$). On CIFAR-100 with ResNet-50, noise+blur achieves 69.23% accuracy vs. 68.4% for JPEG and 67.9% for geometric transforms. The consistency loss is relatively robust to perturbation choice, though noise+blur provides the best trade-off, likely because these perturbations are semantically mild yet sufficiently diverse.

6. Conclusion

We presented *MaCS* (Margin and Consistency Supervision), a simple regularization framework that jointly enforces logit-space separation and local prediction stability. Our theoretical analysis reveals that the *margin-to-sensitivity ratio* governs both generalization and certified robustness, providing a unified view of why both components contribute to improved performance. Extensive experiments across six datasets and seven architectures demonstrate that *MaCS* consistently improves calibration (up to 87% ECE reduction) and corruption robustness while preserving or improving accuracy. Importantly, these gains persist after post-hoc temperature scaling and generalize to corruption types not seen during training.

MaCS requires no additional data, no architectural changes, and adds $\sim 2\times$ training overhead with zero inference overhead, making it an effective drop-in replacement for standard cross-entropy training. The complementarity with AugMix suggests *MaCS* can serve as a base layer for more sophisticated robustness pipelines.

Limitations. (1) Three hyperparameters ($\Delta, \lambda_m, \lambda_c$) may require tuning for significantly different domains. (2) Experiments focus on CIFAR-scale and fine-grained datasets; ImageNet-scale validation remains future work. (3) The consistency loss operates on softmax probabilities, creating a theory-practice gap we bridge empirically but not formally. (4) *MaCS* shows smaller gains on compact architectures (MobileNetV3), suggesting sufficient capacity is needed. Future work includes adaptive loss scheduling, alternative perturbations, ImageNet evaluation, and exploring connections to certified robustness methods.

References

- Bartlett, P. L. The sample complexity of pattern classification with neural networks: the size of the weights is more important than the size of the network. *IEEE Transactions on Information Theory*, 44(2):525–536, 1998.
- Bartlett, P. L., Foster, D. J., and Telgarsky, M. J. Spectrally-normalized margin bounds for neural networks. In *NeurIPS*, pp. 6240–6249, 2017.
- Berthelot, D., Carlini, N., Goodfellow, I., Papernot, N., Oliver, A., and Raffel, C. A. Mixmatch: A holistic approach to semi-supervised learning. In *NeurIPS*, pp. 5049–5059, 2019.
- Bossard, L., Guillaumin, M., and Van Gool, L. Food-101—mining discriminative components with random forests. In *ECCV*, pp. 446–461, 2014.
- Cohen, J., Rosenfeld, E., and Kolter, Z. Certified adversarial robustness via randomized smoothing. In *ICML*, pp. 1310–1320, 2019.
- Deng, J., Guo, J., Xue, N., and Zafeiriou, S. Arcface: Additive angular margin loss for deep face recognition. In *CVPR*, pp. 4690–4699, 2019.
- Dosovitskiy, A., Beyer, L., Kolesnikov, A., Weissenborn, D., Zhai, X., Unterthiner, T., Dehghani, M., Minderer, M., Heigold, G., Gelly, S., et al. An image is worth 16x16 words: Transformers for image recognition at scale. In *ICLR*, 2021.
- Elsayed, G., Krishnan, D., Mobahi, H., Regan, K., and Bengio, S. Large margin deep networks for classification. In *NeurIPS*, pp. 842–852, 2018.
- French, G., Mackiewicz, M., and Fisher, M. Self-ensembling for visual domain adaptation. In *ICLR*, 2018.
- Guo, C., Pleiss, G., Sun, Y., and Weinberger, K. Q. On calibration of modern neural networks. In *ICML*, pp. 1321–1330, 2017.
- He, K., Zhang, X., Ren, S., and Sun, J. Deep residual learning for image recognition. In *CVPR*, pp. 770–778, 2016.
- Hendrycks, D. and Dietterich, T. Benchmarking neural network robustness to common corruptions and perturbations. *ICLR*, 2019.
- Hendrycks, D., Mu, N., Cubuk, E. D., Zoph, B., Gilmer, J., and Lakshminarayanan, B. Augmix: A simple data processing method to improve robustness and uncertainty. In *International Conference on Learning Representations (ICLR)*, 2020.
- Hendrycks, D., Basart, S., Mu, N., Kadavath, S., Wang, F., Dorber, E., Desai, R., Zhu, T., Parajuli, S., Guo, M., et al. The many faces of robustness: A critical analysis of out-of-distribution generalization. In *ICCV*, 2021.
- Hendrycks, D., Zou, A., Mazeika, M., Tang, L., Li, B., Song, D., and Steinhardt, J. PixMix: Dreamlike pictures comprehensively improve safety measures. In *CVPR*, 2022.
- Hinton, G., Vinyals, O., and Dean, J. Distilling the knowledge in a neural network. *arXiv preprint arXiv:1503.02531*, 2015.
- Howard, A., Sandler, M., Chu, G., Chen, L.-C., Chen, B., Tan, M., Wang, W., Zhu, Y., Pang, R., Vasudevan, V., et al. Searching for mobilenetv3. In *ICCV*, pp. 1314–1324, 2019.
- Huang, Z., Bao, X., Zhang, N., Zhang, Q., Tu, X., Wu, B., and Yang, X. Ipmix: Label-preserving data augmentation method for training robust classifiers. *Advances in Neural Information Processing Systems*, 36:63660–63673, 2023.
- Krizhevsky, A., Hinton, G., et al. Learning multiple layers of features from tiny images. Technical report, University of Toronto, 2009.
- Kumar, A., Sarawagi, S., and Jain, U. Trainable calibration measures for neural networks from kernel mean embeddings. In *ICML*, pp. 2805–2814, 2018.
- Lecuyer, M., Atlidakis, V., Geambasu, R., Hsu, D., and Jana, S. Certified robustness to adversarial examples with differential privacy. In *IEEE S&P*, pp. 656–672, 2019.
- Lin, T.-Y., Goyal, P., Girshick, R., He, K., and Dollár, P. Focal loss for dense object detection. In *ICCV*, pp. 2980–2988, 2017.
- Liu, W., Wen, Y., Yu, Z., Li, M., Raj, B., and Song, L. Sphreface: Deep hypersphere embedding for face recognition. In *CVPR*, pp. 212–220, 2017.
- Liu, Z., Lin, Y., Cao, Y., Hu, H., Wei, Y., Zhang, Z., Lin, S., and Guo, B. Swin transformer: Hierarchical vision transformer using shifted windows. In *ICCV*, pp. 10012–10022, 2021.
- Liu, Z., Mao, H., Wu, C.-Y., Feichtenhofer, C., Darrell, T., and Xie, S. A convnet for the 2020s. In *CVPR*, pp. 11976–11986, 2022.
- Madry, A., Makelov, A., Schmidt, L., Tsipras, D., and Vladu, A. Towards deep learning models resistant to adversarial attacks. In *ICLR*, 2018.

- Miyato, T., Maeda, S.-i., Koyama, M., and Ishii, S. Virtual adversarial training: a regularization method for supervised and semi-supervised learning. *IEEE Transactions on Pattern Analysis and Machine Intelligence*, 41(8):1979–1993, 2019.
- Mukhoti, J., Kulharia, V., Sanber, A., Studer, T., Torr, P. H., and Chen, Y. Calibrating deep neural networks using focal loss. In *NeurIPS*, pp. 15288–15299, 2020.
- Naeni, M. P., Cooper, G., and Hauskrecht, M. Obtaining well calibrated probabilities using bayesian binning. In *AAAI*, pp. 2901–2907, 2015.
- Netzer, Y., Wang, T., Coates, A., Bissacco, A., Wu, B., and Ng, A. Y. Reading digits in natural images with unsupervised feature learning. In *NIPS Workshop on Deep Learning and Unsupervised Feature Learning*, 2011.
- Nilsback, M.-E. and Zisserman, A. Automated flower classification over a large number of classes. In *ICVGIP*, pp. 722–729, 2008.
- Parkhi, O. M., Vedaldi, A., Zisserman, A., and Jawahar, C. Cats and dogs. In *CVPR*, pp. 3498–3505, 2012.
- Qin, Y., Zhang, C., Chen, T., Lakshminarayanan, B., Beutel, A., and Wang, X. Understanding and improving robustness of vision transformers through patch-based negative augmentation. *Advances in Neural Information Processing Systems*, 35:16276–16289, 2022.
- Sohn, K., Berthelot, D., Carlini, N., Zhang, Z., Zhang, H., Raffel, C. A., Cubuk, E. D., Kurakin, A., and Li, C.-L. Fixmatch: Simplifying semi-supervised learning with consistency and confidence. In *NeurIPS*, pp. 596–608, 2020.
- Szegedy, C., Zaremba, W., Sutskever, I., Bruna, J., Erhan, D., Goodfellow, I., and Fergus, R. Intriguing properties of neural networks. In *ICLR*, 2014.
- Szegedy, C., Vanhoucke, V., Ioffe, S., Shlens, J., and Wojna, Z. Rethinking the inception architecture for computer vision. In *CVPR*, pp. 2818–2826, 2016.
- Tan, M. and Le, Q. Efficientnet: Rethinking model scaling for convolutional neural networks. In *ICML*, pp. 6105–6114, 2019.
- Thulasidasan, S., Chennupati, G., Bilmes, J., Bhattacharya, T., and Michalak, S. On mixup training: Improved calibration and predictive uncertainty for deep neural networks. In *NeurIPS*, pp. 13888–13899, 2019.
- Tsiligkaridis, T. and Tsiligkaridis, A. Diverse gaussian noise consistency regularization for robustness and uncertainty calibration. In *2023 International Joint Conference on Neural Networks (IJCNN)*, pp. 01–08. IEEE, 2023.
- Tsuzuku, Y., Sato, I., and Sugiyama, M. Lipschitz-margin training: Scalable certification of perturbation invariance for deep neural networks. In *NeurIPS*, 2018.
- Vapnik, V. N. *Statistical learning theory*. Wiley, 1998.
- Wang, H., Wang, Y., Zhou, Z., Ji, X., Gong, D., Zhou, J., Li, Z., and Liu, W. Cosface: Large margin cosine loss for deep face recognition. In *CVPR*, pp. 5265–5274, 2018.
- Wang, H., Xiao, C., Kossaifi, J., Yu, Z., Anandkumar, A., and Wang, Z. AugMax: Adversarial composition of random augmentations for robust training. In *NeurIPS*, 2021.
- Xie, Q., Luong, M.-T., Hovy, E., and Le, Q. V. Self-training with noisy student improves imagenet classification. In *CVPR*, pp. 10687–10698, 2020.
- Zhai, R., Cai, T., He, D., Dan, C., He, K., Hopcroft, J., and Wang, L. MACER: Attack-free and scalable robust training via maximizing certified radius. In *ICLR*, 2020.
- Zhang, H., Cisse, M., Dauphin, Y. N., and Lopez-Paz, D. mixup: Beyond empirical risk minimization. In *ICLR*, 2018.
- Zhang, H., Yu, Y., Jiao, J., Xing, E., El Ghaoui, L., and Jordan, M. Theoretically principled trade-off between robustness and accuracy. In *International conference on machine learning*, pp. 7472–7482. PMLR, 2019.